INTERNATIONAL JOURNAL OF CLIMATOLOGY
Int. J. Climatol. (2010)
Published online in Wiley Online Library
(wileyonlinelibrary.com) DOI: 10.1002/joc.2222

RMetS
Royal Meteorological Society

Satellite monitoring of summer heat waves in the Paris metropolitan area

Bénédicte Dousset,[a,b]* Françoise Gourmelon,[b] Karine Laaidi,[c] Abdelkrim Zeghnoun,[c] Emmanuel Giraudet,[b] Philippe Bretin,[c] Elena Mauri[d] and Stéphanie Vandentorren,[c]

[a] *Hawaii Institute of Geophysics and Planetology, University of Hawaii, Honolulu, Hawaii, USA*
[b] *Géomer, UMR-6554 LETG CNRS, IUEM Plouzané, France*
[c] *Institut de Veille Sanitaire, Saint Maurice, France*
[d] *Istituto Nazionale di Oceanografica e di Geofisica Sperimentale, Trieste, Italy*

ABSTRACT: Summer warming trends in Western Europe are increasing the incidence, intensity and duration of heat waves. They are especially deadly in large cities owing to population density, physical surface properties, anthropogenic heat and pollutants. In August 2003, for 9 consecutive days, the Paris metropolitan area experienced an extreme heat wave that caused 4867 estimated heat-related deaths. A set of 61 NOAA-AVHRR (advanced very high-resolution radiometer) images and one SPOT-high resolution visible (HRV) image were used to analyse the spatial variations of land surface temperature (LST) over the diurnal cycle during the heat wave. The LST patterns were markedly different between daytime and night-time. A heat island was centred downtown at night, whereas multiple temperature anomalies were scattered in the industrial suburbs during the day. The heat wave corresponded to elevated nocturnal LST compared to normal summers. The highest mortality ratios matched the spatial distribution of the highest night-time LSTs, but were not related to the highest daytime LSTs. LSTs were sampled from images at the addresses of 482 elderly people (half were deceased persons and half were control ones) to produce daily and cumulative minimal, maximal and mean thermal indicators, over various periods of time. These indicators were integrated into a conditional logistic regression model to test their use as heat exposure indicators, based on risk factors. Over the period 1–13 August, thermal indicators taking into account minimum nocturnal temperatures averaged over 7 days or over the whole period were significantly linked to mortality. These results show the extent of the spatial variability in urban climate variables and the impact of night-time temperatures on excess mortality. These results should be used to inform policy and contingency planning in relation to heat waves, and highlight the role that satellite remote sensing can play in documenting and preventing heat-related mortality. Copyright © 2010 Royal Meteorological Society

KEY WORDS urban climatology; heat waves; satellite thermal IR sensing; heat stress; mortality

Received 28 December 2009; Revised 30 July 2010; Accepted 08 August 2010

1. Introduction

Observations and reconstructions of global temperature evolution indicate a pronounced warming during the last 150 years, with an increase in the occurrence of so-called heat waves, which are extended periods of anomalously high summertime temperatures (Schär *et al*., 2004). In the last decade, numerous heat waves occurred in Western and Central Europe and in the Mediterranean regions (2003, 2006 and 2007). Climate models for the 21st century suggest that the year-to-year variability of summer temperatures might experience a pronounced increase in response to greenhouse gases, affecting the frequency, intensity and duration of heat waves (Meelh and Tebaldi, 2004; Tebaldi *et al*., 2006). By the end of the century, if greenhouse gas emissions are not reduced, the fraction of days with temperatures above 30 °C in France might equal that currently experienced further south in Spain and in Sicily (Beniston *et al*., 2007).

Heat waves are especially deadly in cities due to population density and urban surface characteristics. Urbanization drastically modifies the partition of the heat fluxes compared to suburban or rural surroundings, generating a differential temperature effect called an *urban heat island*. The main contributing factors are (1) changes in the physical characteristics of the surface such as *albedo*, emissivity or thermal conductivity owing to the replacement of vegetation by asphalt and concrete, and consequently changes in the radiative fluxes; (2) a decrease in surface moisture available for evapotranspiration; (3) changes in the near-surface flow, owing to the complicated geometry of streets and tall buildings; and (4) anthropogenic heat. At night, urban areas gradually release the heat accumulated in structures during the day, whereas rural areas cool off by unobstructed outgoing radiation. As is demonstrated below, it is the lack of relief at night, rather

* Correspondence to: Bénédicte Dousset, Hawaii Institute of Geophysics and Planetology, School of Ocean and Earth Science and Technology, University of Hawaii at Manoa, 680 East-West Road, Honolulu, Hawaii 96822, USA. E-mail: bdousset@hawaii.edu

than high daytime temperatures, that threatens people's health. The elderly, infants, young children, and people with chronic health problems such as asthma and cardiac diseases are more vulnerable. Air pollution, enhanced by high temperatures, further exacerbates the adverse health effects by stressing the respiratory and circulatory systems (Basu and Samet, 2002).

In August 2003, a persistent anticyclone over Western Europe blocked rain-bearing depressions from the Atlantic Ocean and advected dry air from Northern Africa. The average summer temperatures exceeded the 1961–1990 mean by ~3 °C, an increase of up to 5 standard deviations (Schär and Jendritzky, 2004). These anomalous conditions resulted in a heat wave of exceptional strength and duration and a death toll estimated to have exceeded 70 000 (Robine *et al*., 2008). In France, this extreme heat wave event was preceded by an unusually warm and dry spring. Rainfall deficit and high net radiation enhanced by clear skies contributed to early green-up and drying of the soil by evapotranspiration (Zaitchik *et al*., 2006; Fischer *et al*., 2007). From March to August, temperatures exceeded the 1971–2000 long-term mean by 4.7 °C in June, 1.8 °C in July and 4.4 °C in August (Bessemoulin *et al*., 2004).

From 4 to 13 August, the Paris metropolitan area experienced 9 consecutive days with maximum air temperatures above 35 °C, reaching 39 °C at the peak of the heat wave on 12 August. Minimum temperatures steadily increased from 20 to 25.7 °C on 11 and 12 August. The atmosphere was very stable, the wind speed fluctuated between 1 and 4 m/s and the relative humidity and potential evapotranspiration were, respectively, below and above those of normal summers. From the start of the heat wave to its peak, the relative humidity decreased from 38% to 18% during daytime, and from 78% to 58% during night-time. Relative humidity regulates the rate of latent heat transfer from the human body, through perspiration, and high humidity augments the likelihood of heat stress and disorders. Clear skies intensified radiative forcing and strong sunlight triggered the photochemical production of ozone and its accumulation (Tressol *et al*., 2008). However, in Paris the levels of humidity or ozone had little influence on the excess mortality, which was mainly attributable to temperature (Filleul *et al*., 2006). The excess mortality reached +141% in the Paris region, resulting in an estimated 4867 heat-related deaths (Hémon and Jougla, 2003). Figure 1 shows the maximum and minimum air surface temperatures and associated mortality rate in summer 2003 in the Paris region. It indicates a short time lag between temperature increase and death, particularly during 11–13 August at the peak of the heat wave.

Summer warming trends and increased weather variability in Western Europe have important implications for human health, particularly in large cities (Kalkstein and Green, 1997). Health risks increase with heat intensity, relative humidity, time exposure and high minimum

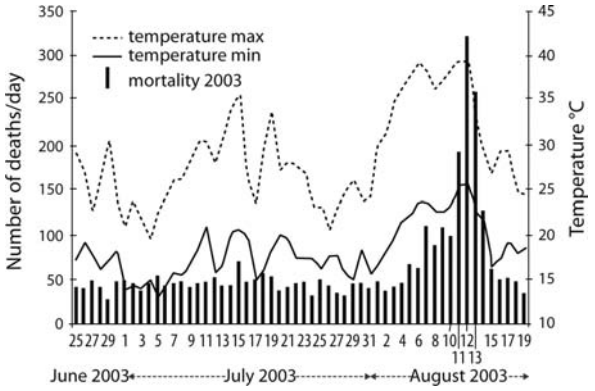

Figure 1. Maximum and minimum surface air temperature at the Paris weather station in the Montsouris Park (right scale) and mortality (left scale), from 25 June to 19 August 2003 (after InVS 2003).

night-time temperatures. Following the 2003 heat wave, the French Institut de Veille Sanitaire (InVS), which is a public health surveillance agency, in cooperation with Météo-France implemented a heat–health warning system based on biometeorological indicators, operating from 1 June to 31 August (Pascal *et al*., 2006). This alert system allows people to enact management and prevention measures when the thresholds are reached. However, the available information does not take into account the intraurban temperature variations, which would enable one to take not only emergency measures but also long-term ones concerning urban planning. For synoptic purposes, most weather stations are situated in parks and airports, away from the effects of built environments. In Paris, the reference weather station is located in the Montsouris Park and its measurements may underestimate the temperatures experienced by people living downtown, or working in suburban industrial areas by several degrees. Furthermore, the weather station network is too sparse to record smaller scale variations in temperatures that may pose an increased risk to human health and which are best resolved using satellite thermal infrared sensing.

Applications of remote sensing in urban climatology have demonstrated the relationship between sprawling conurbations and complex patterns of surface temperature and heat islands (Dousset and Gourmelon, 2003; Streutker, 2003; Kato and Yamaguchi, 2005; Nichol, 2005; Hung *et al*., 2006). Satellite monitoring of extreme heat events in urban areas (Dousset *et al*., 2007; Cheval *et al*., 2009) and estimations of associated public health impact (Johnson *et al*., 2009) are recent developments. The objectives of this research were first, to monitor and analyse the spatial gradient of radiometric surface temperature over the diurnal cycle during the 2003 heat wave; second, to implement indicators of heat exposure for the elderly to better represent the risks of heat stress and mortality and third, to demonstrate the use of satellites for monitoring summer heat waves. This article is divided into four parts. Data acquisition and processing are described in part two. The LST spatial variability over the diurnal cycle, the comparison with the summer

of 1998, the relation to land use/cover, and new indicators of heat exposure are presented in part three. The results are discussed in part four.

2. Methods

2.1. The Paris metropolitan area

Paris (2° 20′E, 48° 50′N) is located in a sedimentary basin on the Seine River. The regional climate is moderated by the oceanic influence of the mid-latitude Westerlies. The Paris Basin is relatively flat with low relief hills, which may produce significant low-level atmospheric motions, although orography has little impact on the thermal parameters (Troude *et al*., 2002). The metropolitan area is characterized by compact urbanization, with a population of nearly 12 million and a high density of ∼20 000 inhabitants/km^2 in the city.

2.2. Remotely sensed data

2.2.1. NOAA-AVHRR acquisition and processing

Two high-resolution thermal images were available during the 4–13 August 2003 heat wave, one from the Landsat-5 Thematic Mapper (TM) (9 August) and another from Terra-ASTER (10 August). However, monitoring requires repetitive imaging to resolve the diurnal cycle and high resolution to observe spatial variability. Geostationary satellites have frequent sampling, but their coarser spatial resolution is insufficient for urban observations. These are best resolved by 1.1-km resolution images from sun-synchronous polar orbiting satellites, such as NOAA, Terra and Acqua, that pass twice daily. In summer 2003, the simultaneous operation of satellites NOAA 12, 16 and 17 provided good coverage with a 4–6 h revisit period.

Eighty-four images, which were sensed from 21 July to 21 August by the advanced very high-resolution radiometer (AVHRR) on board NOAA satellites, were acquired by the high-resolution picture transmission (HRPT) receiving station at the Istituto Nazionale di Oceanografica e di Geofisica Sperimentale, in Trieste. Seventy-six scenes were selected according to clear sky, image quality and small satellite-zenith viewing angle to ensure ground resolution close to 1.1 km and minimize both atmospheric attenuation and anisotropic effects. The images were geometrically corrected for earth rotation and curvature, orthorectified and interactively referenced to a Lambert projection. The AVHRR scans in six spectral channels centred at 0.62 µm (ch. 1), 0.91 µm (ch. 2), 1.61 µm (ch. 3A) and 3.74 µm (ch. 3B), 10.8 µm (ch. 4) and 12 µm (ch. 5). Land albedo and daytime cloudiness were derived from channel 2, and night-time cloudiness from the difference between channels 3 and 4. Cloudy pixels were flagged according to a threshold derived from the histograms of cloud-free images. Normalized difference vegetation indices (NDVI) were computed from the visible and near-infrared channels (ch. 1 and ch. 2). Calibrated brightness temperature was inferred using the internal black-body references of the satellites. The main constraints in retrieving LST from infrared satellite images are (1) the partial absorption of black-body radiation by water vapour and other gases in the atmosphere; (2) the surface emissivities being less than 1 and spatially and spectrally variable (Becker and Li, 1995; Dash *et al*., 2002; Gustafson *et al*., 2006); (3) sub-pixel variations of surface temperature and hot spots averaged nonlinearly through Planck's law (Dozier, 1981, Dousset *et al*., 1993); (4) urban canyons trapping radiant and incident energy, increasing the pixel-averaged emissivity and (5) directional and anisotropic effects due to satellite viewing angles and urban structures (Voogt and Oke, 1998; Lagouarde *et al*., 2004).

In August 2003, the air was dry and the differential atmospheric attenuation from thermal channels 4 and 5 yielded negligible water vapour corrections equivalent to errors less than 1 °C at night and 1 °C to 1.7 °C during the day for brightness temperatures between 30 and 40 °C, respectively. Uncertainties related to radiosounding and modelling of atmospheric transmittance to account for atmospheric absorption would exceed actual errors, and this correction was not justified. The correction for time-independent emissivity was also neglected, because the objective was to study the relative temporal variations of surface temperatures. Most images with satellite-zenith angles higher than 35° were rejected; however, a few were kept and empirically corrected based on consecutive images with smaller satellite-zenith angles (Roujean *et al*., 1997; Lagouarde *et al*., 2004). Median LST images were constructed from 50 NOAA-AVHRR images over six time intervals of satellites passes (i.e. 1–3, 4–7, 9–12, 12–15, 15–18 and 20–23 UTC) during the 9-day heat wave episode. Figure 2 shows the diurnal distribution of the 50 images, and Figure 3 displays the six median LST images, each averaged over six to ten individual images.

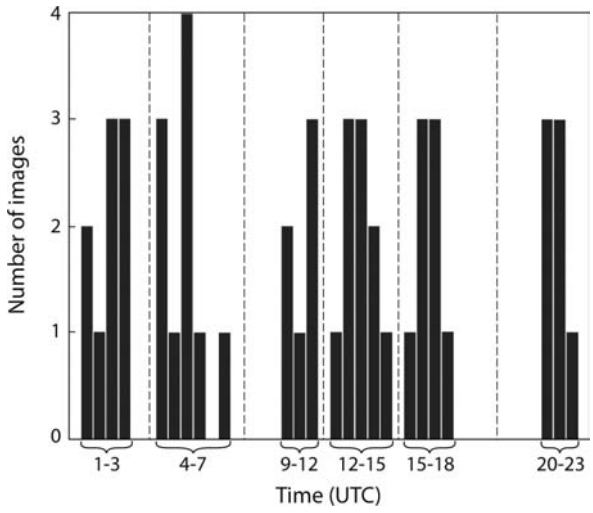

Figure 2. Temporal distribution of 50 images sensed by NOAA satellites 12, 16 and 17 over the region of Paris from 4 to 13 August 2003.

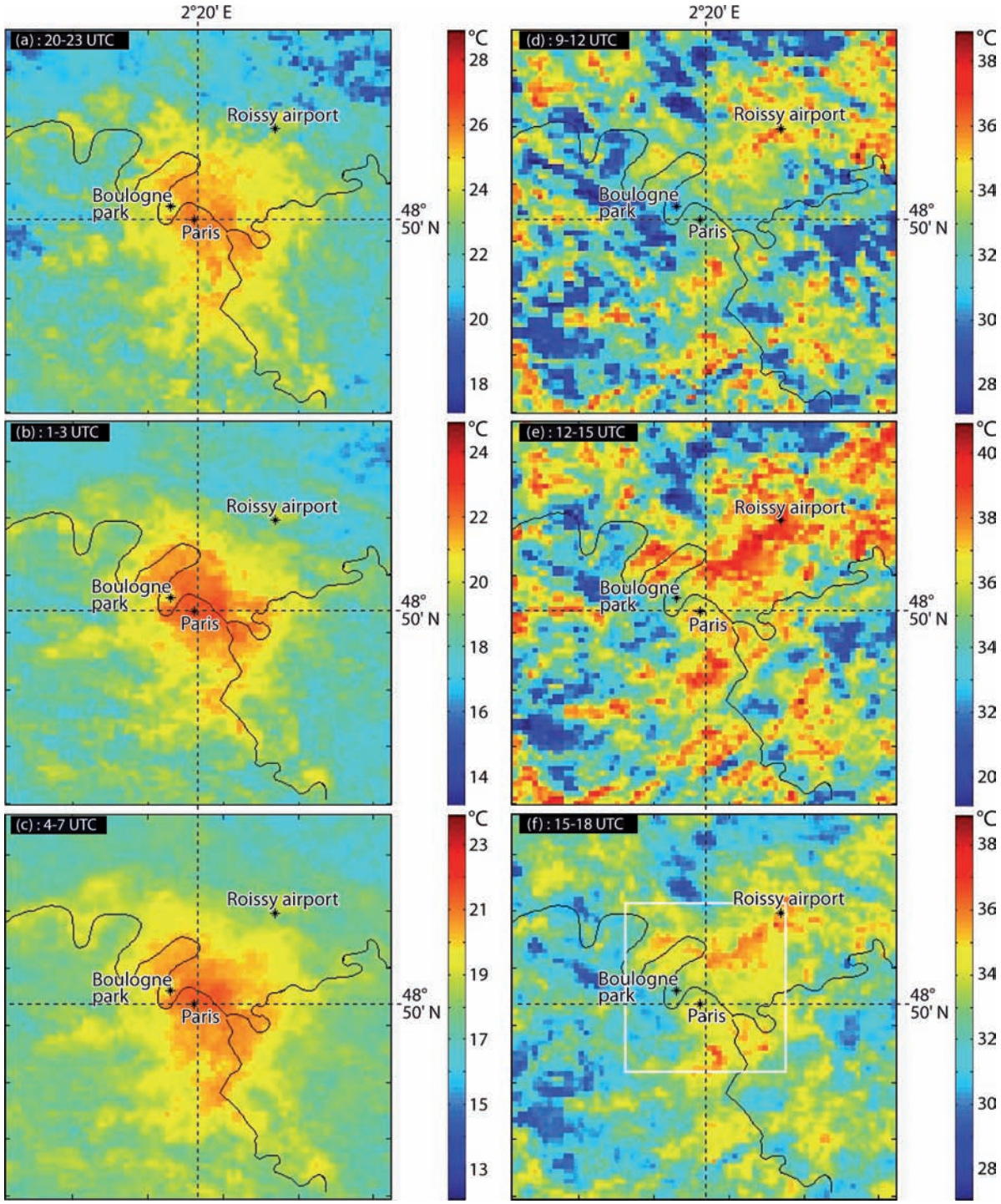

Figure 3. Average LST infrared images (see text) from 4 to 13 August 2003, for each of the diurnal time intervals shown in Figure 2. The colour scale (in degrees Celsius) is optimally enhanced separately for each image. The white square represents the enlarged area of Figure 4(a).

2.2.2. *SPOT HRV -4 acquisition and processing*

Surface characteristics and properties that govern the surface energy balance were extracted from a SPOT-4HRV multi-spectral image acquired on 13 July 2003, three weeks before the extreme event. The processing of the SPOT image included detector radiometric equalization, geometric processing to remove the earth rotation and resampling across-track to a uniform 20-m pixel size. Figure 4(a) represents the unsupervised land cover classification derived from the four visible and near-infrared channels, which yielded six classes corresponding to water, densely built urban areas, sub-urban residential areas, light bare soils, forest and lawns and fields. The classification was further validated using the NDVI, calculated from the SPOT visible and near-infrared channels. A geographic information system (GIS) was used to generate land use/cover fractional images and merge 20-m SPOT and 1-km AVHRR pixels. Ancillary data on urban administrative delineations,

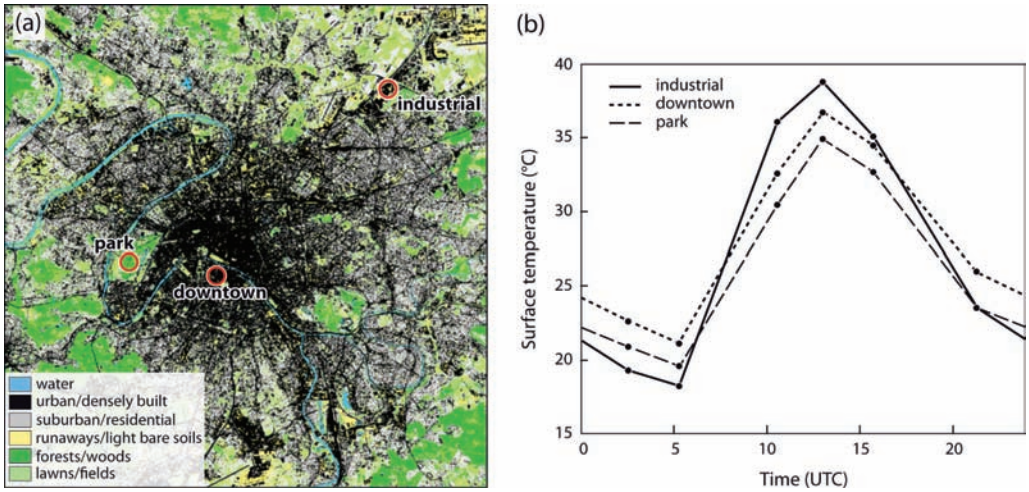

Figure 4. (a) Land cover classification of Paris derived from a SPOT-4 HRV image on 13 July 2003. The three locations used to construct the mean diurnal cycles of land surface temperature (LST) shown in (b) are indicated by circles. (b) Mean diurnal cycles of LST, constructed from 50 NOAA-AVHRR images, at an industrial site, in downtown Paris, and in an urban park (4–13 August 2003).

parks, rivers and industrial areas were obtained from the Paris Department of Planning (APUR) and integrated in the GIS database.

2.3. *In situ* meteorological data

The *in situ* meteorological data were recorded at the Paris automated weather station in Montsouris Park. Hourly data include surface air temperature (T_{air}) at 10 cm, 50 cm and 1.50 m above the surface, ground temperature at −10 cm, dew-point, wind speed and direction, relative humidity, water vapour and insolation and net radiation. Additional data at 00 : 12 UTC include ground temperatures at −20 cm, −50 cm and −1 m depth. Colocated *in situ* and remotely sensed data from Montsouris Park were used to interpret LST results, taking into account the different nature of these measurements.

2.4. Public health data

Following the summer of 2003, the InVS conducted a case–control study to identify the mortality risk factors for elderly people living in the Paris region during the heat wave (Ledrans *et al*., 2005; Vandentorren *et al*., 2006). The study included 241 people aged 65 and over, who died between 8 and 13 August and remained at home for at least 24 h before death or hospitalization. These 241 cases were matched with 241 controls, who were people living in a district of Paris under similar socio-economic conditions, having the same sex and age class as the cases, but survived the heat wave (Ledrans *et al*., 2005). The surface temperature near the domicile of the considered cases and controls was one of the many risk factors related to death that were investigated. Other factors included age, sex, socio-economic conditions, family entourage, behaviour during the heat wave, mobility, health status, housing conditions and environment. In the previous work, LSTs on 200-m radius around the 482 addresses were derived from a single Landsat TM image at 10 : 17 UT on 9 August. Although the spatial resolution of this image is very high, this timing was not optimal to assess thermal patterns. Because the 16-day repeat cycle of the Landsat image precludes daily monitoring, thermal indices for this study were estimated from a time series of 61 NOAA-AVHRR images (1–13 August). The thermal index of an address corresponds to the LST of the pixel that contains the address. Different indicators of temperature exposure were constructed based on minimum and maximum LST, taking into account different lags between temperature and death, and daily temperatures as well as temperatures averaged over 3, 7 and 13 days, based on the knowledge of the lag between temperature extremum and health impact. These indicators were alternately integrated into the conditional logistic model of the previous case–control study, replacing the single indicator. This conditional logistic model (Breslow and Day, 1980) was adjusted for the same variables as in the previous study (age, sex, etc.) so that the relationship between thermal indicators and mortality could be tested.

3. Results

3.1. The LST diurnal cycle

Figure 3 shows six composite images of median LST, constructed from 50 images taken between 4 and 13 August. The LST spatial variability over the diurnal cycle is evident. The images reveal contrasting daytime and night-time heat island patterns, reflecting the different day and night rates of heating and cooling between urban and suburban areas, enhanced by the stable atmosphere that characterized the heat wave episode. The LST variability was analysed as a function of urban surface characteristics by merging data from the 20-m resolution classified SPOT image, and from APUR, with the 1-km resolution NOAA-AVHRR images (Dousset and Gourmelon, 2003).

At night-time, the images show strong urban heat islands of up to 8 °C over the 20–23 UTC and 1–3 UTC averaging periods (Figure 3(a) and (b)), and up to 6 °C over 4–7 UTC (Figure 3(c)). The LST distribution was well correlated with increasing built density from the suburbs to downtown. At the peak of the heat wave, low relative humidity of 27–40% in the evenings (20–23 UTC) in Montsouris Park suggests that vegetated areas in the residential suburbs and rural areas may have been conducive to evaporative and radiative cooling. In the rural areas north of Paris, LST decreased by ∼4 °C, and remained constant the rest of the night. In downtown Paris, temperatures decreased slowly as the heat stored in buildings and trapped in urban 'canyons' was progressively lost and anthropogenic heat was continually produced. Eventually, the LST decreased after sunrise, both in the suburbs (∼19 °C) and downtown (∼22 °C) (Figure3(c)).

During the daytime, multiple temperature anomalies were scattered in the densely built and industrial suburbs, conveying mostly variations of the surface heat balance between dry and comparatively moist surfaces. In Montsouris Park, relative humidity dropped from 38% to 18% at the peak of the heat wave, and the wind fluctuated between ∼0 and 2 m/s. From 9 to 12 UTC, the northeast region quickly warmed because of unobstructed field of view, low thermal inertia surfaces and anthropogenic heat produced by heavy traffic and industries. From 12 to 15 UTC (Figure 3(e)), heat islands up to 11 °C were observed between the industrial suburbs and the forests. The highest LSTs of 38–42 °C occurred in the suburbs: to the north in the industrial areas of St. Ouen, Aubervilliers, St. Denis and in the freight zones of Le Bourget, Garonord and Roissy airport; to the west in the industrial area of Argenteuil and to the south in the freight and industrial areas of Ivry-sur-Seine and the Orly airport.

Figure 4(b) displays the diurnal cycle of mean LST at three locations: downtown Paris, Garonord (industries near Roissy Airport) and the Boulogne park, shown in Figure 4(a). Urban canyons in downtown Paris consist of asphalt pavement, stone or concrete buildings of up to 7–10 floors and roofed with slate or zinc. The industrial area comprises large warehouses of 2–3 levels, with corrugated steel or fibre roofs, asphalt or concrete parking lots, and roads. The ∼8 km^2 Boulogne Park is mainly composed of lawns, trees, bushes and a small lake. The mean diurnal cycles indicate a near-constant difference of ∼1.5–2.2 °C between downtown and the park, but differences of +3 °C at night, and −3.5 °C at noon between downtown and the industrial area, and +4.5 °C at noon between the industrial area and the park (Figure 5). The industrial surfaces with lower thermal inertia and unobstructed sky view are consistently warmer at daytime and cooler at night-time than the downtown and park surfaces.

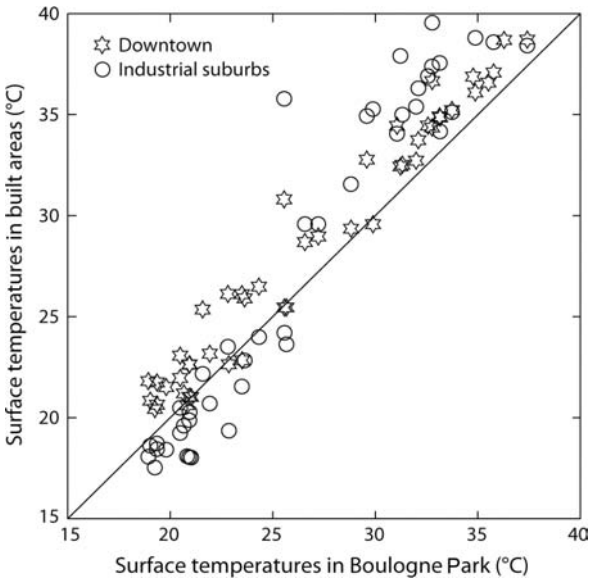

Figure 5. Scatter plot of satellite LSTs of built areas (contrasting downtown and industrial suburbs) against satellite LSTs in the Bois de Boulogne Park taken as reference.

3.2. Colocated satellite and *in situ* data in Montsouris Park

T_{air} and LST measurements are intrinsically different. The former corresponds to the ambient temperature at 1.50 m above the surface, whereas the latter represents the surface radiometric temperature averaged over a pixel, mostly composed of horizontal surfaces within different levels of the canopy layer. These measurements are complementary, because the sensible heat flux is determined by the temperature difference between the surface and the air immediately above it. Their correlation arises from the surface heat balance.

Figure 6(a) shows an hourly time series of T_{air} at 1.50 m and LST at the 4–6 h satellite sampling interval. Figure 6(b) and (c) shows the hourly time series of relative humidity and wind speed. Figure 6(d) and (e) shows the scatter plots of satellite LST *versus* T_{air} at night (01–06 UTC) and by day (12–15 UTC) for 1–13 August. Slopes and offsets of the linear regressions are shown in the respective figures. The linear correlation coefficient was 0.92 at night, but only 0.68 during the day, presumably reflecting stronger sub-pixel variations of surface cover and heat balance regimes. Minima of both T_{air} and LST occurred before sunrise at ∼05:00 UTC, just before insolation resumed and net radiation ceased to be negative. At night, T_{air} was generally 1–2 °C higher than LST, except on 12 August at the peak of the heat wave, when the near-surface gradient reached 5 °C presumably because of lack of mixing. Maximum LSTs occurred at the time of maximum solar irradiance, while maximum T_{air} lagged typically by ∼3 h. At ∼13:00 UTC, T_{air}-LST varied from −2 to −4 °C, implying a significant near-surface temperature gradient due to intense radiative heating. Some residual difference may also be attributed to the effects of the satellite viewing geometry (Lagouarde *et al.*, 2004).

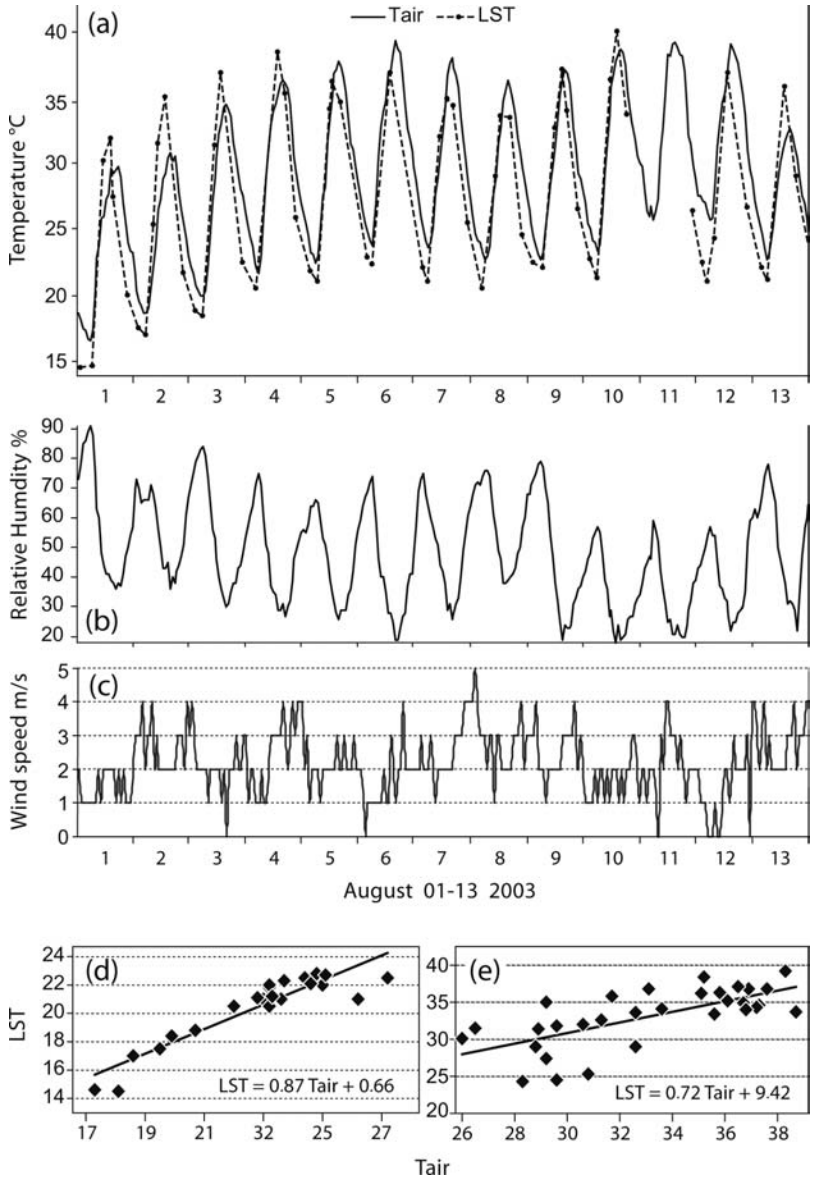

Figure 6. Colocated satellite and *in situ* data from the weather station in the Montsouris Park: (a) hourly T_{air} at 1.50 m and LST at the 4–6-h satellite sampling interval, (b) hourly relative humidity, (c) wind speed, (d) scatter plots of satellite LST *versus* T_{air} at night *(01–06 UTC),* (e) and at daytime (12–15 UTC) for 1–13 August. Mid-day LST appears lower than T_{air} for 5–8 August due to a lack of data.

3.3. LST comparison of the August 2003 heat wave with August 1998

The time series of images of August 2003 were compared with those of August 1998, previously analysed by Dousset and Gourmelon (2003). The comparison indicates a large difference in the vegetation indices and high minimum temperatures. The metropolitan area is surrounded by fields and forests, and the city comprises a dozen small parks (0.1–0.6 km^2), and two large ones (8–10 km^2) at the west and east edges. In spring 2003, strong incident radiation and large precipitation deficit forced an early spring green-up and progressively reduced the soil moisture. Consequently, the vegetation index of August 2003 is lower than normal summers and evidences a significantly increased drought and reduced primary productivity (Ciais *et al*., 2005; Zaitchik *et al*., 2006). Figure 7 represents the bivariate histogram of the composite afternoon LST (12–15 UTC) *versus* the mean NDVI for 4–13 August 2003 (a) and its distribution (b). The figure indicates a significant negative correlation with a slope of $\sim -0.2\,^{\circ}$C/%NDVI that illustrates the importance of vegetation in the partitioning between latent and sensible surface heat fluxes. Analysis and manual sampling of individual images indicate that the LST is 2–3 °C lower in small parks than in their built surroundings and 4–5 °C lower in large ones.

Figure 8 shows median LST diurnal cycles over the Paris metropolitan area, one from 5 to 11 August 1998, and the other from 1 to 13 August 2003. In 1998, the period from 5–11 August was relatively warm, with area-mean maximum LSTs between 28 and 36 °C, and LSTs for 4 consecutive days were over 35 °C. However, the highest area-mean minimum LSTs never exceeded 15 °C, thus averting the occurrence of a heat wave. In 2003,

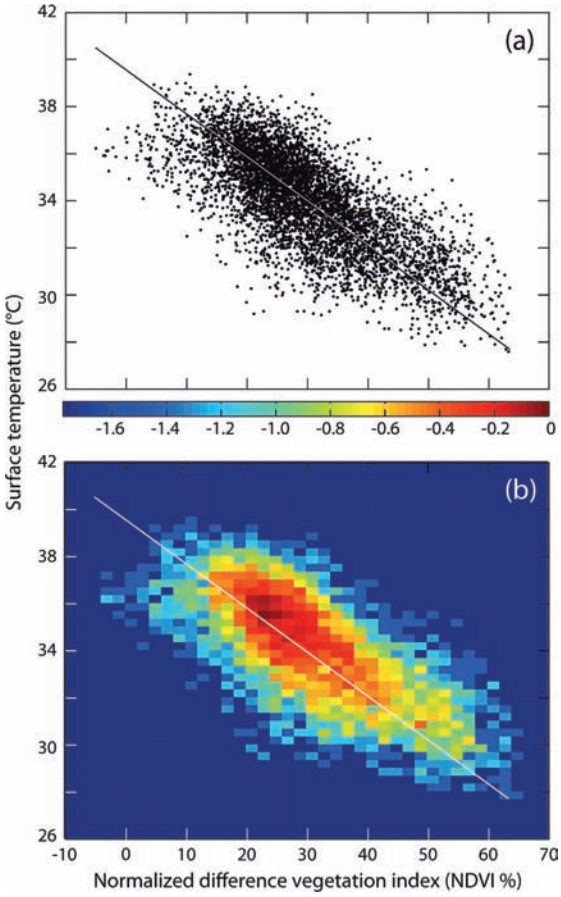

Figure 7. Scatter plot and bivariate histogram of LST-averaged 12–15 UTC (4–13 August 2003) *versus* the averaged NDVI. The colour bar shows the log 10 of the bivariate distribution normalized by the largest value. The principal mode of variance has a slope of −0.186 °C/%NDVI.

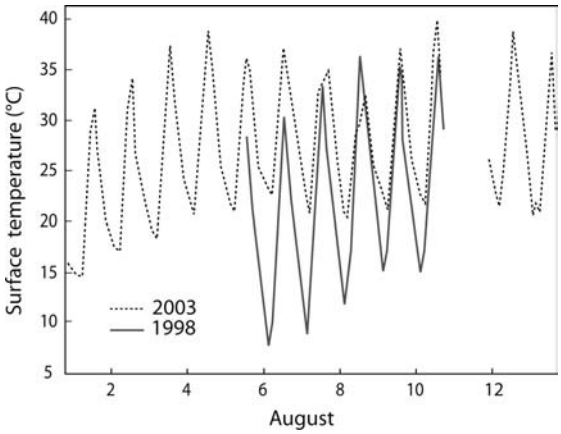

Figure 8. Median LST diurnal cycles over the Paris metropolitan area, from 5 to 11 August 1998, and from 1 to 13 August 2003. Mid-day LSTs that appear lower on 7–9 August 2003 than 1998 are due to a lack of data.

the diurnal amplitude was 5 °C lower (16 °C *vs* 21 °C) than that in 1998, and the mean minimum was 8 °C higher which confirms the impact of night-time minimum temperature on the heat wave. For two consecutive nights, on 10–11 and 11–12 August, stable meteorological conditions and low winds prevented convective mixing. At 05 : 00 UTC (07 : 00 local time), the minimum T_{air} was 25.7 °C for both nights. On 11 August, night-time LSTs were still 21.5 °C in Montsouris Park and 25–26 °C in downtown Paris. These high minimum night-time temperatures contributed to a lack of night rest for vulnerable people and to 500 excess deaths in the Paris region, on these two particularly deadly days during the heat wave (Figure 1). On the 13th, both temperatures and mortality excess began to decrease, and returned to normal on the 19th.

3.4. LST and mortality

Multilayer maps were generated over the six composite thermal images to identify risk factor areas. Standard layers, which were selected first, included surface albedo, percentage of built and vegetated surfaces, hydrology, population density, industrial areas and transportation.

Figure 9(a) represents the LST from 01 to 03 UTC and Figure 9(b) that of 12 to 15 UTC, with some of the land use overlays. Although the 1-km spatial resolution of the infrared images may be coarse for urban climate analysis, the overlays demonstrate the high sensitivity of the signal, such as a 1.5 °C decrease or increase attributable to the Jardin des Plantes Park and to the Palais du Louvre, respectively. At night, in the 20–22 UTC and 0–3 UTC composite images, the spatial distribution of the highest LSTs of 24 °C to 26 °C in the districts south and northeast of the Seine River matched the spatial distribution of the highest mortality ratios described in Cadot and Spira (2006), which were not related to the highest daytime LSTs. These maps would be useful for taking preventive measures to reduce strenuous activities in industrial areas north of Paris, where LST reached 40 °C in the afternoon, and assist elderly people living in the southern districts, where LST remained 25 °C at night.

Figure 10 displays the spatial distribution of the 482 cases and control addresses over Paris and the department of Val de Marne, in the suburbs of Paris. A total of ∼29 000 individual LST measurements were extracted at these addresses, using 61 satellite images recorded between 1 and 13 August.

Table I lists the adjusted odds ratio (OR) of mortality for the different thermal indicators (OR adjusted on age, sex, socio-economic conditions, family entourage, behaviour during the heat wave, mobility, health status, housing conditions, and so on). The OR is a relative measure of risk, which indicates the probability for someone exposed to a given factor to develop the outcome, as compared to someone with less or no exposure. If exposure is not linked to health impact, the OR is close to 1. If exposure is positively linked to health impact, OR >1. If exposure is negatively linked to health impact (protective effect), then OR <1. OR is given with a confidence interval (CI): if the value 1 is included in the CI, the result is not statistically significant. Table I shows that thermal indicators taking the average or maximum daytime temperatures into account were not significantly

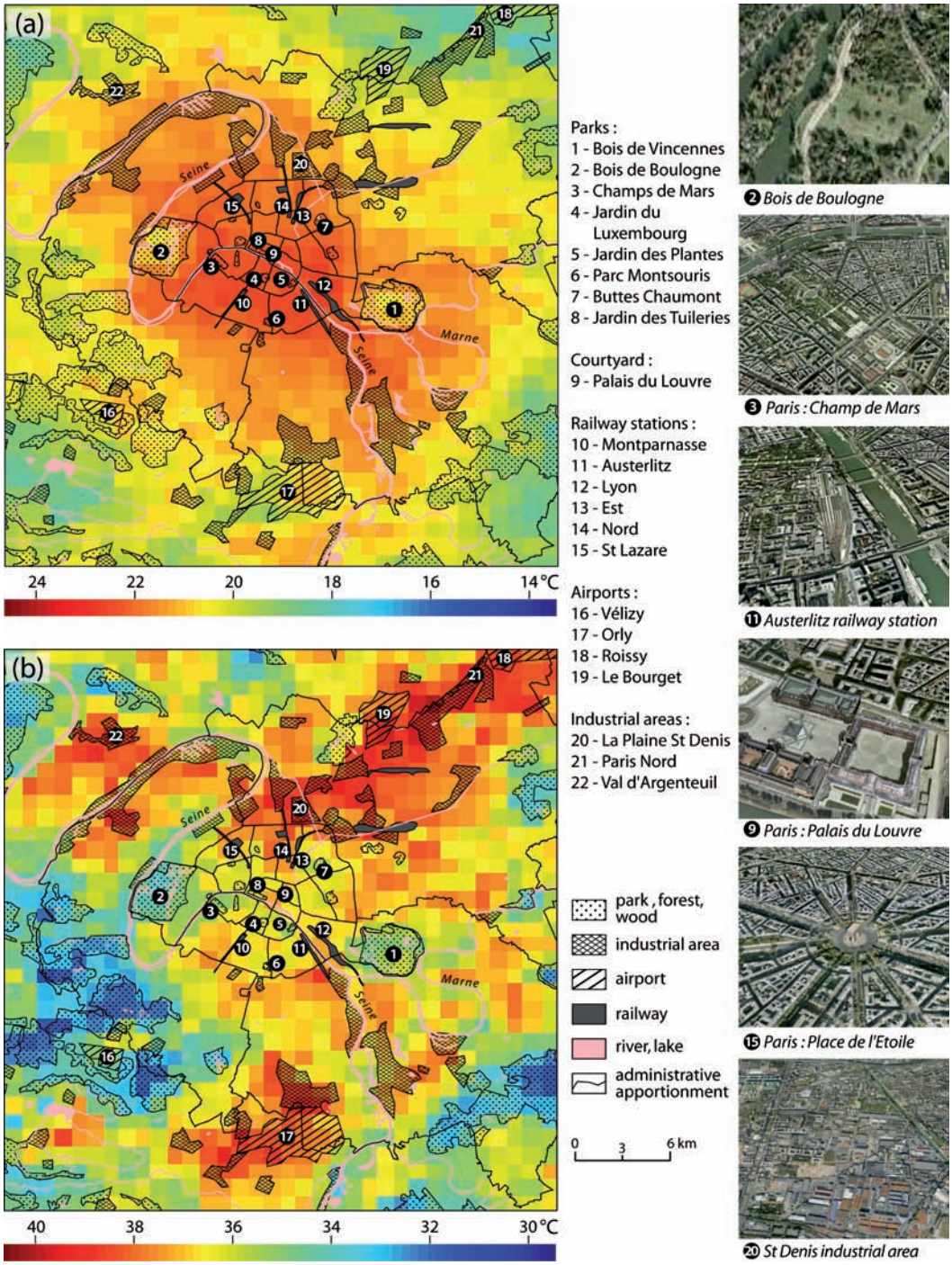

Figure 9. LST composite images of the Paris region from NOAA-AVHRR, under a land cover/use information layer; (a) at night (01–03 UTC); (b) by day (12–15 UTC). The thumbnail pictures display areas cooler and warmer than their surroundings (images from 2010 Aerodata International Survey, Google 2009).

linked to deaths. However, those taking minimum nocturnal temperatures into account were significantly linked to death. For example, for the mean minimum nocturnal temperature in the 7-day interval until the date of death, the OR associated with a 0.5 °C LST difference between cases and controls was 2.2, indicating a death risk more than twice as high. This value of 0.5 °C corresponds to the 90th percentile of the distribution of the differences between the cases and controls for this indicator.

4. Discussion and conclusion

This study documented the satellite monitoring of a 9-day heat wave over a metropolitan area and the associated epidemiological risk and time lag of death for elderly persons at given locations. The thermal images showed contrasting night-time and daytime heat island patterns, which were related to surface characteristics and land uses. The results confirm the influence of nocturnal temperatures on heat wave intensity and excess mortality,

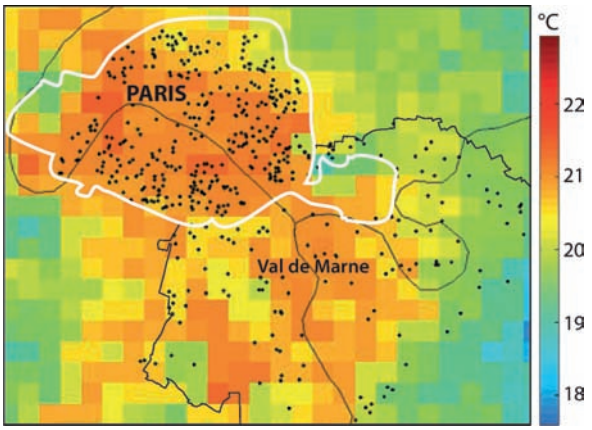

Figure 10. Spatial distribution of the 482 cases and control addresses in Paris and the Val de Marne department, over the NOAA-AVHRR thermal image of 7 August at 04 : 50 UTC.

Table I. Results of the logistic model showing adjusted odds ratios of mortality for different thermal indicators. The rows *italicized* indicate significant results. The odds ratios were adjusted for age, sex, socio-economic conditions, family entourage, behaviour during heat wave, mobility, health status and housing conditions.

Land surface temperature indicators from NOAA-AVHRR images	OR (Cl 95%)
Mean of the minimal temperatures for 7 days (day of death and 6 preceding days)	*2.22 (1.03–4.81)*
Mean of the maximal temperatures for 7 days (day of death and 6 preceding days)	0.96 (0.69–1.33)
Mean of the minimal temperatures from 1 to 13 August	*2.57 (1.17–5.64)*
Mean of the maximal temperatures from 1 to 13 August	1.14 (0.77–1.67)
Mean of the average temperatures from 1 to 13 August	2.07 (0.91–4.70)

OR, odds ratio; Cl 95%, 95% confidence interval.

and show the contribution of urban heat islands in intensifying the heat wave by absorbing heat during the day and progressively raising minimum nocturnal temperatures linked with heat stress and mortality. Urban parks had a significant impact on surface temperature with a 0.2 °C LST decrease per %NDVI, despite a prior warm and dry spring that lowered moisture availability.

The effect of urban heat islands on mortality is well known and the variability of death risk within cities has been investigated (Canouï-Poitrine *et al.*, 2006). Some studies (Vandentorren *et al.*, 2006; Johnson *et al.*, 2009) have integrated societal factors with LST derived from a single Landsat TM image. This study, consisting of the joint analysis of a large time series of thermal images and of colocated validated cases of elderly mortality, allowed us to infer the relative impact of heat exposure on elderly population at given locations and assess the time lag between heat exposure and death. It demonstrated the predominance of mean minimum nocturnal temperature, where a 0.5 °C increase doubles the risk of death, in the temperature range of the heat wave period.

There are implications regarding temperature monitoring and public health surveillance that are key issues in Europe given the summer warming trend and the resulting increase in heat wave incidence, duration and intensity, and also the aging of the population, which brings greater physiological and social vulnerability. Heat-related deaths are more frequent in large cities. In France, in 2003, the excess mortality was 40% in small towns, but 80% in Lyon and 141% in Paris (Vandentorren *et al.*, 2004). An analogous heat wave in USA would result in a mortality rate of +150% for New York City (Kalkstein *et al.*, 2008).

Satellite monitoring of summer heat waves provides surface temperature values that can be merged with urban databases to identify risk areas at the scale of a district or a neighbourhood, and supply criteria for adaptation strategies. Satellite monitoring can provide data to substantially improve understanding of urban surface processes and societal vulnerabilities to near-term climatic changes. Although Paris was chosen as a case study, having recently experienced an extreme heat wave with well-documented health consequences, the methods used in this study are general and should be applicable to other cities as well.

Acknowledgements

This work was funded by the MAIF Foundation. B. Dousset was partially supported by a National Research Council scholarship at the National Oceanic and Atmospheric Administration, Air Resources Laboratory (Silver Spring). Land-cover layers were supplied by the Atelier Parisien d'Urbanisme. Discussions with Julian Wang and Dian Seidel are gratefully acknowledged. Nancy Hulbirt prepared the figures. Contribution number 7995 of the School of Ocean and Earth Sciences and Technology, University of Hawaii.

References

Basu R, Samet JM. 2002. Relation between elevated ambient temperature and mortality: a review of the epidemiologic evidence. *Epidemiologic Reviews* **24**: 190–202.

Becker F, Li ZL. 1995. Surface temperature and emissivity at various scales: definition, measurements and related problems. *Remote Sensing Reviews* **12**: 225–253.

Beniston M, Stephenson DB, Christensen OB, Ferro CAT, Frei C, Goyette S, Halsnaes K, Holt T, Jylhä K, Koffi B, Palutikof J, Schöll R, Semmler T, Woth K. 2007. Future extreme events in European climate: an exploration of regional climate model projections. *Climatic Change* **81**: 71–95.

Bessemoulin P, Bourdetee N, Courtier P. 2004. La canicule d'août 2003 en France et en Europe. *La Météorologie* **46**: 25–33.

Breslow NE, Day NE. 1980. Statistical methods in cancer research. Vol. 1- the analysis of case control studies. *IARC Scientific Publications* **32**: 5–338.

Cadot E, Spira A. 2006. Canicule et surmortalité à Paris en août 2003, le poids des facteurs socio-économiques. *Espace Populations et Sociétés* **2–3**: 239–249.

Canouï-Poitrine F, Cadot E, Spira A. 2006. Excess deaths during the August 2003 heat wave in Paris, France. *Revue d Epidemiologie et de Sante Publique* **54**(2): 127–135.

Cheval S, Dumitrescu A, Bell A. 2009. The urban heat island of Bucharest during the extreme high temperatures of July 2007. *Theoretical and Applied Climatology* **97**(3–4): 391–401.

Ciais P, Reichstein M, Viovy N, Granier A, Ogée J, Allard V, Aubinet M, Buchmann N, Bernhofer C, Carrara A, Chevallier F, De Noblet N, Friend AD, Friedlingstein P, Grünwald T, Heinesch B, Keronen P, Knohl A, Krinner G, Loustau D, Manca G, Matteucci G, Miglietta F, Ourcival JM, Papale D, Pilegard K, Rambal S, Seufert G, Soussana JF, Sanz MJ, Schulze ED, Vesala T, Valentini R. 2005. Europe-wide reduction in primary productivity caused by the heat and drought in 2003. *Nature* **437**: 529–533.

Dash P, Göttsche FM, Olesen FS, Fischer H. 2002. Land surface temperature and emissivity estimation from passive sensor data: theory and practice – current trends. *International Journal of Remote Sensing* **23**(13): 2563–2594.

Dousset B, Flament P, Bernstein R. 1993. Los Angeles fires seen from space. *EOS Transactions-American Geophysical Union* **74**: 33, 37–38.

Dousset B, Gourmelon F. 2003. Satellite multi-sensor data analysis of urban surface temperatures and land cover. *ISPRS Journal of Photogrammetry and Remote Sensing* **58**: 43–54.

Dousset B, Gourmelon F, Mauri E. 2007. Application of satellite Remote Sensing for Urban Risk Analysis: a case study of the 2003 extreme heat wave in Paris. *Urban Remote Sensing Joint Event* **11–13**: 1–5, DOI: 10.1109/URS.2007.371849.

Dozier J. 1981. A method for satellite identification of surface temperature fields of subpixel resolution. *Remote Sensing of Environment* **11**: 221–229.

Filleul L, Cassadou S, Medina S, Fabres P, Lefranc A, Eilstein D, Le Tertre A, Pascal L, Chardon B, Blanchard M, Declercq C, Jusot JF, Prouvost H, Ledrans M. 2006. The relation between temperature, ozone, and mortality in nine French cities during the heat wave of 2003. *Environmental Health Perspectives* **114**(9): 1344–1347.

Fischer EM, Seneviratne SI, Vidale PL, Lüthi D, Schär C. 2007. Soil moisture – atmosphere interactions during the 2003 European Summer Heat Wave. *Journal of Climate* **20**: 5081–5099.

Gustafson WT, Gillespie AR, Yamada GJ. 2006. Revisions to the ASTER temperature/emissivity separation algorithm. *2nd International Symposium on Recent Advances in Quantitative Remote Sensing*. Global Change Unit, University of Valencia: Torrent, Spain.

Hémon D, Jougla E. 2003. Surmortalité liée à la canicule d'août 2003. Rapport d'étape. Estimation de la surmortalité et principales caractéristiques épidémiologiques. Inserm; 59.

Hung T, Uchihama D, Ochi S, Yasuoka Y. 2006. Assessment with satellite data of the urban heat island effects in Asian megacities. *International Journal of Applied Earth Observation and Geoinformation* **8**(1): 34–48.

Johnson D, Wilson JS, Luber GC. 2009. Socioeconomic indicators of heat-related health risk supplemented with remotely sensed data. *International Journal of Health Geographics* **8**: 57, DOI: 10.1186/1476-072X-8-57.

Kalkstein LS, Green JS. 1997. An evaluation of climate/mortality relationships in large U.S cities and the possible impacts of climate change. *Environmental Health Perspectives* **105**: 84–93.

Kalkstein LS, Greene JS, Mills DM, Perrin AD, Samenow JP, Cohen JC. 2008. Analog European heat waves for U.S. cities to analyze impacts on heat-related mortality. *Bulletin of the American Meteorological Society* **89**: 75–85.

Kato S, Yamaguchi Y. 2005. Analysis of urban heat-island effect using ASTER and ETM+ Data: Separation of anthropogenic heat discharge and natural heat radiation from sensible heat flux. *Remote Sensing of Environment* **99**: 44–54.

Lagouarde JP, Moreau P, Irvine M, Bonnefond JM, Voogt JA, Solliec F. 2004. Airborne experimental measurements of the angular variations in surface temperature over urban areas: case study of Marseilles (France). *Remote Sensing of Environment* **93**: 443–462.

Ledrans M, Vandentorren S, Bretin P, Croisier A. 2005. Etude des facteurs de risque de dècés des personnes agées résidant à domicile durant la vague de chaleur d'août 2003. Rapport de l'Institut national de Veille Sanitaire. pp 1–116. ISBN: 2-11-094963-5.

Meelh GA, Tebaldi C. 2004. More Intense, more frequent, and longer lasting heat waves in the 21st century. *Science* **305**: 5686, 994–997.

Nichol JE. 2005. Remote sensing of urban heat islands by day and night. *Photogrammetric Engineering and Remote Sensing* **71**: 613–623.

Pascal M, Laaidi K, Ledrans M, Baffert E, Caserio-Schönemann C, Le Tertre A, Manach J, Medina S, Rudant J, Empereur-Bissonnet P. 2006. France's heat health watch warning system. *International Journal of Biometeorology* **50**: 144–153.

Robine JM, Cheung S, Le Roy S, Van Oyen H, Griffiths C, Michel JC, Herrmann F. 2008. Death toll exceeded 70,000 in Europe during the summer of 2003. *CR Biology* **331**: 171–178.

Roujean JL, Tanré D, Bréon FM, Deuzé JL. 1997. Retrieval of land surface parameters from airborne POLDER bidirectional reflectance distribution function during HAPEX-Sahel. *Journal of Geophysical Research* **102**: 11201–11218.

Shär C, Jendritzky G. 2004. Climate change: Hot news from summer 2003. *Nature* **432**: 559–560.

Schär C, Vidale PL, Luthi D, Frei C, Haberli C, Liniger MA, Appenzeller C. 2004. The role of increasing temperature variability in European summer heat waves. *Nature* **427**: 332–336.

Streutker DR. 2003. Satellite-measured growth of the urban heat island of Houston, Texas. *Remote Sensing of Environment* **85**: 282–289.

Tebaldi C, Hayhoe K, Arblaster JM, Meehl GA. 2006. Going to extreme. *Climatic Change* **79**: 185–211.

Tressol M, Ordonez C, Zbinden R, Brioude J, Thouret V, Mari C, Nedelec P, Cammas JP, Smit H, Patz HM, Volz-Thomas A. 2008. Air pollution during the 2003 European heat wave as seen by MOZAIC airliners. *Atmospheric Chemistry and Physics* **8**: 2133–2150.

Troude F, Dupont E, Carissimo B, Flossmann A. 2002. Relative influence of urban and orographic effects for low wind conditions in the Paris area. *Boundary-Layer Meteorology* **103**: 493–505.

Vandentorren S, Bretin P, Zeghnoun A, Mandereau-Bruno L, Croisier A, Cochet C, Ribéron J, Siberan I, Declercq B, Ledrans M. 2006. August 2003 heat wave in France: risk factors for death of elderly people living at home. *European Journal of Public Health* **16**: 583–591.

Vandentorren S, Suzan F, Medina S, Pascal S, Maulpoix A, Cohen JC, Ledrans M. 2004. Mortality in 13 French Cities during the August 2003 heat wave. *American Journal of Public Health* **94**: 1518–1520.

Voogt JA, Oke TR. 1998. Effects of urban surface geometry on remotely sensed surface temperature. *International Journal of Remote Sensing* **19**: 895–920.

Zaitchik BF, Macalady AK, Bonneau LR, Smith RB. 2006. Europe's 2003 heat wave: a satellite view of impacts and land-atmosphere feedbacks. *International Journal of Climatology* **26**: 743–769.

